Development 136, 1363-1374 (2009) doi:10.1242/dev.031872

Map2k1 and *Map2k2* genes contribute to the normal development of syncytiotrophoblasts during placentation

Valérie Nadeau*, Stéphanie Guillemette*, Louis-François Bélanger, Olivier Jacob, Sophie Roy and Jean Charron†

The mammalian genome contains two ERK/MAP kinase kinase genes, *Map2k1* and *Map2k2*, which encode dual-specificity kinases responsible for ERK/MAP kinase activation. In the mouse, loss of *Map2k1* function causes embryonic lethality, whereas *Map2k2* mutants survive with a normal lifespan, suggesting that *Map2k1* masks the phenotype due to the *Map2k2* mutation. To uncover the specific function of MAP2K2 and the threshold requirement of MAP2K proteins during embryo formation, we have successively ablated the *Map2k* gene functions. We report here that *Map2k2* haploinsufficiency affects the normal development of placenta in the absence of one *Map2k1* allele. Most *Map2k1*$^{+/-}$*Map2k2*$^{+/-}$ embryos die during gestation because of placenta defects restricted to extra-embryonic tissues. The impaired viability of *Map2k1*$^{+/-}$*Map2k2*$^{+/-}$ embryos can be rescued when the *Map2k1* deletion is restricted to the embryonic tissues. The severity of the placenta phenotype is dependent on the number of *Map2k* mutant alleles, the deletion of the *Map2k1* allele being more deleterious. Moreover, the deletion of one or both *Map2k2* alleles in the context of one null *Map2k1* allele leads to the formation of multinucleated trophoblast giant (MTG) cells. Genetic experiments indicate that these structures are derived from *Gcm1*-expressing syncytiotrophoblasts (SynT), which are affected in their ability to form the uniform SynT layer II lining the maternal sinuses. Thus, even though *Map2k1* plays a predominant role, these results enlighten the function of *Map2k2* in placenta development.

KEY WORDS: MAP2K1 kinase, MAP2K2 kinase, ERK/MAPK cascade, Conditional deletion, Placenta, Labyrinth morphogenesis

INTRODUCTION

Mitogen-activated protein kinase (MAPK) signaling pathways consist in protein kinase cascades linking extracellular stimuli with various targets scattered in the different cell compartments (Rubinfeld and Seger, 2005; Seger and Krebs, 1995). The classical ERK/MAPK pathway, which appears to be the major one in growth factor signaling, involves the extracellular-signal-regulated kinases ERK1 and ERK2 (renamed MAPK3 and MAPK1, respectively) and the ERK kinases (MAP2K1 and MAP2K2, also known as MEK1 and MEK2). MAP2K1 and MAP2K2 are dual-specificity kinases that activate MAPK1 and MAPK3 upon agonist binding to receptors (Crews et al., 1992). The ERK/MAPK pathway is implicated in cell-fate determination in *Caenorhabditis elegans*, *Drosophila melanogaster* and *Xenopus laevis* (Hsu and Perrimon, 1994; Kornfeld et al., 1995; Umbhauer et al., 1995; Wu et al., 1995). In mammals, this cascade plays a crucial role in development, including fate determination, differentiation, proliferation, survival, migration, growth and apoptosis (Fischer et al., 2005; Johnson and Vaillancourt, 1994; Ussar and Voss, 2004).

Although two different MAP2K proteins are present in the ERK/MAPK cascade in mammals, a single *Map2k* gene fulfills this role in *C. elegans*, *D. melanogaster* and *X. laevis*. Sequence analysis revealed that the murine MAP2K1 is more related to the *X. laevis* MAP2K1 (X-MEK) than to the mouse MAP2K2 (see Fig. S1 in the supplementary material) (Brott et al., 1993; Crews et al., 1992; Russell et al., 1995). MAP2K2 protein is 80% identical and 90% similar to MAP2K1, whereas X-MEK presents 91% identity and 96% similarity to murine MAP2K1. Two short regions of MAP2K1 show reduced homology with MAP2K2: (1) the amino-terminus (25% identical/53% similar over 36 residues), and (2) the proline-rich insert (17% identical/33% similar over 18 residues). These two motifs are essential for MAP2K function, as they affect the efficiency of ERK phosphorylation, the phosphorylation of residue Ser386 of MAP2K1/2 by MAPK1/3, and the subcellular localization of MAP2K1/2 (Rubinfeld and Seger, 2005). The amino-terminus of MAP2K1/2 proteins contains the MAPK1/3 docking site and a nuclear export sequence. The proline-rich domain is shared by MAP2K proteins from different species (see Fig. S1B in the supplementary material) (Dang et al., 1998). The proline-rich domain of MAP2K1 contains a PAK phosphorylation site (Ser298) important for its function (Coles and Shaw, 2002). This domain is also involved in the interaction with the Raf family members (Catling et al., 1995; Dang et al., 1998; Eblen et al., 2002; Nantel et al., 1998; Papin et al., 1996). In vitro, PAK phosphorylation of MAP2K1 on residue Ser298 stimulates MAP2K1 autophosphorylation on the activation loop, which leads to the phosphorylation of MAPK1/3 by MAP2K1. Although Ser298 is present in MAP2K2, MAP2K2 is a poor substrate of PAK1 (Frost et al., 1997; Park et al., 2007). In addition, the Thr residues found at positions 286 and 292 of MAP2K1, which are involved in feedback regulation of the ERK/MAPK cascade once phosphorylated, are not conserved in MAP2K2 (Rubinfeld and Seger, 2005). Thus, protein sequence differences between MAP2K1 and MAP2K2 suggest that these two proteins have diverged to achieve unique functions in mammals.

A differential response of MAP2K1 and MAP2K2 to certain stimuli also exists. For instance, only MAP2K1 is activated in Swiss 3T3 and macrophage cells in response to bombesin and tumor necrosis factor α, respectively (Seufferlein et al., 1996;

Centre de recherche en cancérologie de l'Université Laval, Centre Hospitalier Universitaire de Québec, L'Hôtel-Dieu de Québec, Québec, QC, G1R 2J6, Canada.

*These authors contributed equally to this work
†Author for correspondence (e-mail: jean.charron@crhdq.ulaval.ca)

Accepted 12 February 2009

Winston et al., 1995). This is further supported by our observations that the ERK/MAPK cascade cannot be activated in response to bombesin in *Map2k1*$^{-/-}$ mouse embryonic fibroblasts (M. Tremblay, S.R. and J.C. unpublished). By contrast, MAP2K2 is specifically activated by lactosylceramide in human aortic smooth muscle cells or by estradiol in mouse cerebral cortex (Bhunia et al., 1996; Setalo et al., 2002). Differential activation of MAP2K1 and MAP2K2 by Raf family members in EGF-stimulated HeLa cells has also been described (Wu et al., 1996). In addition, only MAP2K1 can form a signaling complex with Ras and c-Raf in serum-stimulated NIH 3T3 cells, suggesting that in these conditions the c-Raf signaling preferentially transits via MAP2K1 (Jelinek et al., 1994). The Rac-PAK pathway has been shown to be involved in the activation of the ERK/MAPK cascade by regulating the formation of a specific MAP2K1-MAPK1/3 signaling complex, which is under the control of PAK and MAPK1/3 phosphorylation sites unique to MAP2K1 in the proline-rich sequence (Eblen et al., 2002; Eblen et al., 2004). Finally, MAP2K1 and MAP2K2 act at different steps during the cell cycle: MAP2K1 provides proliferative signals whereas MAP2K2 induces growth arrest at the G1/S boundary (Ussar and Voss, 2004). The role of MAP2K1 in proliferation seems to depend on its ability to translocate MAPK1 to the nucleus following MAP2K1 Thr292 and Ser298 phosphorylation (Skarpen et al., 2007). Altogether these data support a model in which the transduction of specific signals transits via distinct protein kinase isoforms through the ERK/MAPK cascade (Acharya et al., 1998). The presence of various isoforms at the different levels of the pathway may reflect the complexity of the controls required for the fine regulation of the multiple processes in mammalian cells.

The differential role of MAP2K1 and MAP2K2 in signal transduction during mouse development was revealed by the characterization of mutant mouse lines in which *Map2k1* and *Map2k2* genes were disrupted (Bélanger et al., 2003; Bissonauth et al., 2006; Giroux et al., 1999). The null mutation of *Map2k1* results in a recessive lethal phenotype, the mutant embryos dying at 10.5 days of gestation (E10.5) due to abnormal placenta development with marked undergrowth of the labyrinth region and reduction of its vascularization. However, *Map2k1*$^{-/-}$ mice survive if the development of the extra-embryonic structures is rescued (Bissonauth et al., 2006). The *Map2k1*$^{-/-}$ phenotype is observed in the presence of normal *Map2k2* expression levels in the placenta providing genetic evidence that *Map2k2* is unable to make up for the absence of *Map2k1* (Giroux et al., 1999). By contrast, *Map2k2*$^{-/-}$ mice show no obvious phenotype, suggesting compensatory effects by *Map2k1* (Bélanger et al., 2003). These data support the idea of an essential role for *Map2k1* during mammalian development.

To circumvent the potential functional redundancy between MAP2K1 and MAP2K2 that precludes the definition of a specific physiological role for MAP2K2 during development, *Map2k* alleles were successively mutated. Mice with combined *Map2k1* and *Map2k2* haploinsufficiency showed reduced survival rate at birth. The *Map2k1*$^{+/-}$*Map2k2*$^{+/-}$ embryos dying during gestation presented an underdevelopment of the placenta labyrinth region and a reduction of its vascularization. The *Map2k1*$^{+/-}$*Map2k2*$^{+/-}$ survival rate can be rescued by restricting the *Map2k1* mutation to the embryo. The placenta phenotype is *Map2k1/Map2k2* gene dosage-dependent with a predominant role of *Map2k1*. *Map2k2* haploinsufficiency in the absence of one *Map2k1* allele also leads to the abnormal differentiation of the syncytiotrophoblast (SynT) layer II and to the accumulation of multinucleated trophoblast giant (MTG) cells.

MATERIALS AND METHODS

Mouse strains and genotyping

All experiments were performed according to the guidelines of the Canadian Council on Animal Care and approved by the institutional animal care committee. The genotyping by Southern blot and PCR analyses of the *Map2k1* and *Map2k2* mutant mouse lines, the *Sox2Cre* deleter mouse line and the *ROSA26 Cre* reporter (*R26R*) mouse line have been previously described (Bélanger et al., 2003; Bissonauth et al., 2006; Giroux et al., 1999; Hayashi et al., 2003; Soriano, 1999). The mouse lines are in the 129/Sv genetic background except the *R26R* line, which is in a 129Sv-C57BL/6 hybrid background. The *Gcm1Cre* deleter mouse line was generated in the laboratory and will be described in detail in a subsequent manuscript.

Histological and immunohistochemical analyses

Specimens were collected and processed for paraffin inclusion. Serial sections of 4 μm were stained according to standard histological procedures to identify specific cell types: Hematoxylin and Eosin, Periodic acid/Schiff (for glycogen trophoblasts) (Schmitz et al., 2007), DAPI/Phalloidin (for multinucleated cells), MSB (martius/scarlet/blue for fibrin deposits) (Lendrum et al., 1962) and alkaline phosphatase (ALP, for SynT) (Bissonauth et al., 2006).

Proliferation was assessed by immunostaining with a rabbit polyclonal antibody against the phosphorylated histone H3 (pH3; Upstate Biotechnology, Lake Placid, NY) (Aubin et al., 2002) and by BrdU labeling. Intraperitoneal injection of BrdU (100 μg/g body weight) was performed 4 hours before sacrifice. BrdU incorporation was detected as described in Hayashi et al. (Hayashi et al., 1988) with some modifications. Paraffin sections were incubated in 1 N HCl for 1 hour at 40°C followed by a trypsin digestion (0.025% w/v) at 40°C for 20 minutes before detection with a mouse monoclonal antibody (1:1000; Chemicon International, Temecula, CA). Apoptotic cells were detected by terminal transferase (TdT) DNA end labeling (TUNEL) according to Giroux and Charron (Giroux and Charron, 1998). The placenta vascular network was revealed with a rat monoclonal antibody against CD31/PECAM (1:50; Pharmingen, Mississauga, ON), whereas MAP2K1 and MAP2K2 were detected using rabbit monoclonal antibodies (1:100 and 1:250, respectively; Epitomics, Burlingame, CA). Antigen retrieval was performed by microwaving samples in 0.01 M citrate buffer at pH 6.0. The Vectastain HRP ABC Reagent (Vector Laboratories, Burlingame, CA) was used for detection and the sections were counterstained with Hematoxylin. For these analyses, at least six specimens per genotype were tested and the most representative fields are presented.

In situ hybridization and β-galactosidase staining

Radioactive in situ hybridization on tissue sections was performed with *Gcm1* and *Tpbpa* [^{35}S]UTP-labeled riboprobes as previously described (Bissonauth et al., 2006; Giroux et al., 1999). β-Galactosidase staining was performed on cryosections. Dissected placentas were fixed in 4% paraformaldehyde/0.2% glutaraldehyde in PBS at 4°C for 25 minutes and 60 minutes for E10.5 and E12.5 specimens, respectively. The placentas were then equilibrated in 30% sucrose in 0.1 M phosphate buffer pH 7.3 overnight at 4°C before embedding in OCT medium. Serial cryosections of 10 μm were postfixed for 5 minutes and X-Gal staining was performed as described (Bissonauth et al., 2006).

Western blot analysis

Protein extracts from E10.5 embryos and from their corresponding placenta were prepared (Bélanger et al., 2003; Bissonauth et al., 2006). Total protein lysates (20 μg) were resolved on denaturing 10% SDS-PAGE and detected with anti-phospho-specific MAPK1/MAPK3 (Cell Signaling Technology Inc., Pickering, ON) and homemade rabbit polyclonal anti-MAP2K1, anti-MAP2K2 and anti-MAPK1 antibodies. At least four specimens per genotype were analyzed. The most representative western blots are presented.

Statistical analyses

For proliferation and apoptosis studies, the ratio of positive cells to total cell number was determined for a minimum of five random areas. Repeated measures for the linear mixed model were performed to assess the difference between genotypes at all stages studied when genotype is considered the

Table 1. Reduced viability of *Map2k1*$^{+/-}$*Map2k2*$^{+/-}$ embryos and mice

Map2k1$^{+/-}$*Map2k2*$^{+/+}$×*Map2k1*$^{+/+}$*Map2k2*$^{-/-}$

			Genotype of live embryos and mice†	
Age*	Number of litters	Number of pups	*Map2k1*$^{+/+}$*Map2k2*$^{+/-}$	*Map2k1*$^{+/-}$*Map2k2*$^{+/-}$
E10.5	7	38	17 (53%)	15 (47%; 6)
E12.5	8	54	27 (59%)	19 (41%; 8)
E14.5	12	49	26 (81%)	6 (19%; 17)
E18.5	5	22	16 (89%)	2 (11%; 4)
W3-4	89	361	329 (91%)	32 (9%)

*E10.5, E12.5, E14.5 and E18.5 represent day 10.5, 12.5, 14.5 and 18.5 of gestation, respectively; W3-4 represents a range in ages of the pups in weeks after birth.
†The percentage of live embryos and the number of dead embryos identified at the different embryonic ages analyzed is indicated.

fixed effect and area the random effect. The procedure PROC MIXED from the SAS System was used (Littell et al., 1998). For the various breedings, deviation to the Mendelian distribution was assessed using χ^2 test.

RESULTS

Map2k2 haploinsufficiency jeopardizes normal embryonic development in the absence of one *Map2k1* allele

To establish if *Map2k2* plays a specific function during mouse development, we investigated the consequences of the lack of *Map2k2* function in the context of a reduced dosage of *Map2k1*. First, *Map2k1*$^{+/-}$ and *Map2k2*$^{-/-}$ mice were intercrossed to generate double heterozygous mutants (*Map2k1*$^{+/-}$*Map2k2*$^{+/-}$; DH). Unexpectedly, among the 361 viable offspring produced, only 32 *Map2k1*$^{+/-}$*Map2k2*$^{+/-}$ mice were obtained at weaning, corresponding to 9% of the progeny instead of the expected 50% Mendelian ratio ($P<10^{-15}$) (Table 1). Thus, the combined loss of one allele of each *Map2k* gene was more deleterious than the *Map2k2* homozygous mutation (Bélanger et al., 2003).

To determine the time of death of the *Map2k1*$^{+/-}$*Map2k2*$^{+/-}$ embryos, *Mak2k1*$^{+/-}$ and *Map2k2*$^{-/-}$ mice were bred and embryos were recovered from E10.5 to E18.5. Mendelian ratios of *Map2k1*$^{+/+}$*Map2k2*$^{+/-}$ and *Map2k1*$^{+/-}$*Map2k2*$^{+/-}$ live embryos were obtained at E10.5 ($P>0.5$) but not at E12.5 ($P<0.08$). From E10.5 onward, a substantial proportion of *Map2k1*$^{+/-}$*Map2k2*$^{+/-}$ embryos was moribund or in the process of being resorbed (Table 1). At E14.5 and E18.5, *Map2k1*$^{+/-}$*Map2k2*$^{+/-}$ embryos constituted only 19% and 11% of the live embryos, respectively ($P<10^{-10}$). Thus, the lethality of the *Map2k1*$^{+/-}$*Map2k2*$^{+/-}$ embryos was detected as early as E10.5, and this phenotype increased with gestational age.

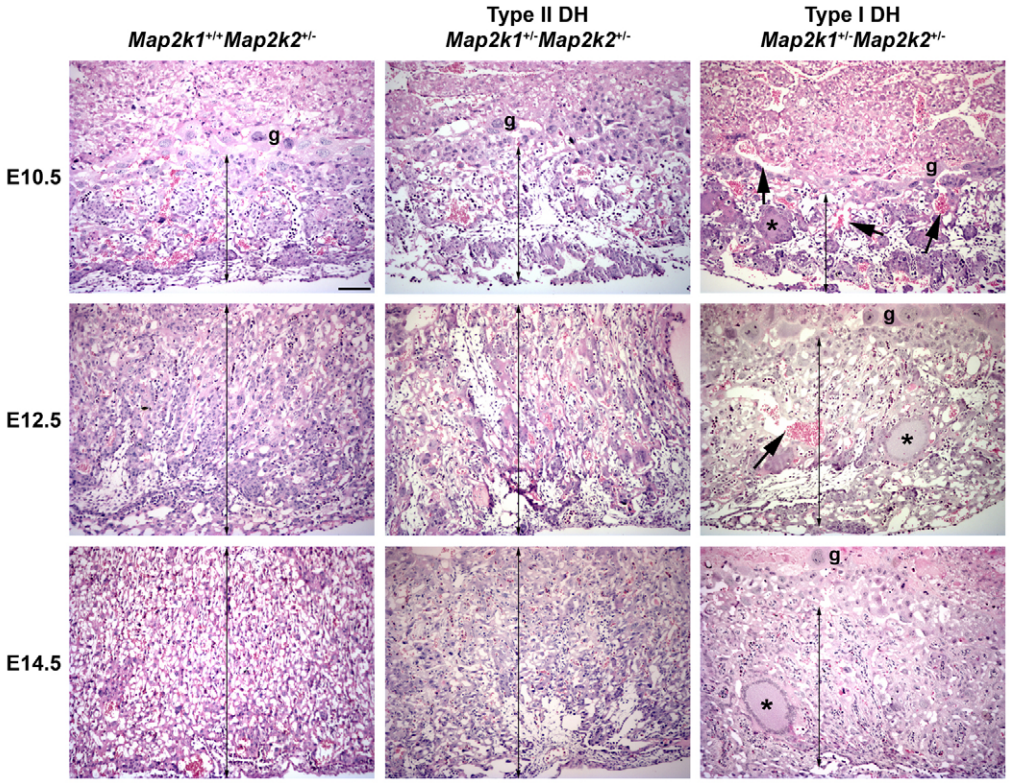

Fig. 1. Underdevelopment of the labyrinth region in the placenta from *Map2k1Map2k2* DH mutants. Hematoxylin and Eosin staining of E10.5, E12.5 and E14.5 control (*Map2k1*$^{+/+}$*Map2k2*$^{+/-}$), type I and type II DH (*Map2k1*$^{+/-}$*Map2k2*$^{+/-}$) placenta sections. The type I DH specimens show a reduction in the thickness of the labyrinth region (double-headed arrowheads). Large maternal blood sinuses (arrows) and MTG cells (*) are also observed in type I DH mutants. Scale bar: 100 μm. g, trophoblast giant cells.

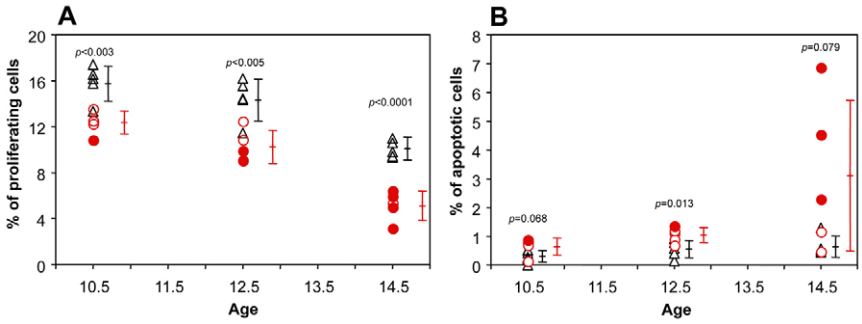

Fig. 2. The underdevelopment of the labyrinth region in *Map2k1*$^{+/-}$*Map2k2*$^{+/-}$ placenta results from reduced proliferation and increased apoptosis. (**A**) Proliferation was assessed by immunostaining with phospho-histone H3 antibody on paraffin sections of E10.5, E12.5 and E14.5 control (*Map2k1*$^{+/+}$*Map2k2*$^{+/-}$), type I and type II DH (*Map2k1*$^{+/-}$*Map2k2*$^{+/-}$) placentas. The percentage of labyrinth trophoblasts in proliferation is presented. A statistically significant reduction in proliferation was observed for type I (filled circles) and type II (open circles) DH placentas when compared with control specimens (triangles) at all ages analyzed. (**B**) Apoptosis was detected by TUNEL assay and the percentage of labyrinth trophoblasts in apoptosis is presented. The apoptotic cell ratio was significantly increased at E12.5 for DH placentas. Moreover, the type I DH mutant (filled circles) showed an important increase in apoptosis at E14.5 when compared with type II DH (open circles) and control specimens (triangles).

Map2k1$^{+/-}$*Map2k2*$^{+/-}$ embryos present placenta defects

The surviving *Map2k1*$^{+/-}$*Map2k2*$^{+/-}$ mice had a normal lifespan and were fertile, reminiscent of our previous observations regarding the *Map2k1*$^{-/-}$ mice when the mutation was not targeted to the extra-embryonic tissues (Bissonauth et al., 2006). To investigate if *Map2k1* and *Map2k2* haploinsufficiency can perturb normal placenta development without directly interfering with embryo formation, we analyzed the placenta of E10.5 to E14.5 conceptuses. As *Map2k1*$^{+/-}$ and *Map2k2*$^{+/-}$ mutants were indistinguishable from their wild-type littermates, *Map2k2*$^{+/-}$ specimens were used as controls and breedings between *Map2k1*$^{+/-}$ and *Map2k2*$^{-/-}$ mice were performed to generate DH mutants (Fig. 4; see Fig. S2 in the supplementary material) (Bélanger et al., 2003; Bissonauth et al., 2006). Histological examination of *Map2k1*$^{+/-}$*Map2k2*$^{+/-}$ specimens at different stages revealed the presence of two categories of mutants (Fig. 1). From E10.5 to E14.5, 25 out of 32 *Map2k1*$^{+/-}$*Map2k2*$^{+/-}$ embryos, hereafter referred to as type I DH mutants, had a small placenta and corresponded to the most affected conceptuses (moribund or resorbed embryos) (Table 4). Histological analyses of type I DH mutant placentas showed a severe reduction of the labyrinth size (Fig. 1). The labyrinth region was compact and disorganized, with numerous empty spaces, large maternal sinuses and aberrant MTG cells. By contrast, the histology of type II DH specimens was similar to that of *Map2k2* heterozygous placentas. Thus, these results implicate *Map2k2* in placenta formation.

The underdevelopment of the labyrinth in *Map2k1*$^{-/-}$ placentas was attributed to the concerted reduction of proliferation and survival of labyrinth trophoblasts (Bissonauth et al., 2006). To verify if these processes were also affected in *Map2k1*$^{+/-}$*Map2k2*$^{+/-}$ placentas, we performed proliferation assays on E10.5 to E14.5 placentas. In control placentas, the proliferation rate in the labyrinth region was elevated as previously observed (Fig. 2A) (Bissonauth et al., 2006). By contrast, the proliferation rate was significantly reduced in *Map2k1*$^{+/-}$*Map2k2*$^{+/-}$ specimens at all ages analyzed (P<0.005). TUNEL assays were also performed to define if increased apoptosis contributed to the reduced *Map2k1*$^{+/-}$*Map2k2*$^{+/-}$ labyrinth region. Very few apoptotic cells were detected in E10.5 to E14.5 control and *Map2k1*$^{+/-}$*Map2k2*$^{+/-}$ placentas, but at E12.5 the augmented number of apoptotic cells in *Map2k1*$^{+/-}$*Map2k2*$^{+/-}$ specimens was statistically significant (P=0.013) (Fig. 2B). Moreover, in all specimens examined apoptosis was more important in type I DH placentas when compared with controls or type II DH mutant placentas, this phenomena being more important at E14.5, suggesting that type I DH embryos might be in the process of being resorbed. Therefore, perturbed cell proliferation may underlie the reduced expansion of the labyrinth region of the placenta from *Map2k1*$^{+/-}$*Map2K2*$^{+/-}$ mutants, whereas augmented apoptosis may be secondary to the resorption process.

The embryonic lethal phenotype of *Map2k1*$^{-/-}$ mutants is due to the underdevelopment of the labyrinth associated with its hypovascularization (Bissonauth et al., 2006). To determine if the reduced survival of the *Map2k1*$^{+/-}$*Map2k2*$^{+/-}$ embryos involved a placenta vascularization defect, we examined the vascular network by using the endothelial cell marker CD31 on sections of E10.5 to E14.5 control and *Map2k1*$^{+/-}$*Map2k2*$^{+/-}$ placentas. In control and type II DH specimens, the fetal blood vessels invaded the whole labyrinth region and the density of blood vessels increased with age (Fig. 3A, not shown). By contrast, the number of embryonic blood vessels was reduced in type I DH placentas, a result clearly seen at E14.5 (Fig. 3A). To visualize the maternal vascular network, we also performed alkaline phosphatase assays to label the differentiated SynT lining the maternal sinuses. A strong staining was detected around the maternal sinuses in both control and type I DH specimens (Fig. 3B). The number of sinuses increased in control placentas with embryonic age, whereas in type I DH specimens sinus formation was significantly reduced at all stages analyzed. These data indicate that the combined *Map2k1Map2k2* haploinsufficiency affects trophoblast proliferation and labyrinth vascularization, as both fetal and maternal vascular networks are perturbed in type I DH mutants. Thus, not only is *Map2k1* required for normal placentation, but *Map2k2* also appears involved in labyrinth growth and morphogenesis.

Rescue of extra-embryonic components restores survival of *Map2k1Map2k2* haploinsufficient conceptuses

To directly address the importance of the placenta defects on survival, we have rescued the placenta phenotype using the *Map2k1* conditional allele (*Map2k1*^{flox} allele) (Bissonauth et al., 2006). *Map2k1*$^{flox/\Delta}$*Map2k2*$^{+/+}$ females were bred with *Map2k1*$^{+/+}$*Map2k2*$^{-/-}$*Tg*$^{+/Sox2Cre}$ males to specifically ablate *Map2k1* function in embryonic derivatives, retaining the undeleted *Map2k1*^{flox} allele in extra-embryonic tissues (Hayashi et al.,

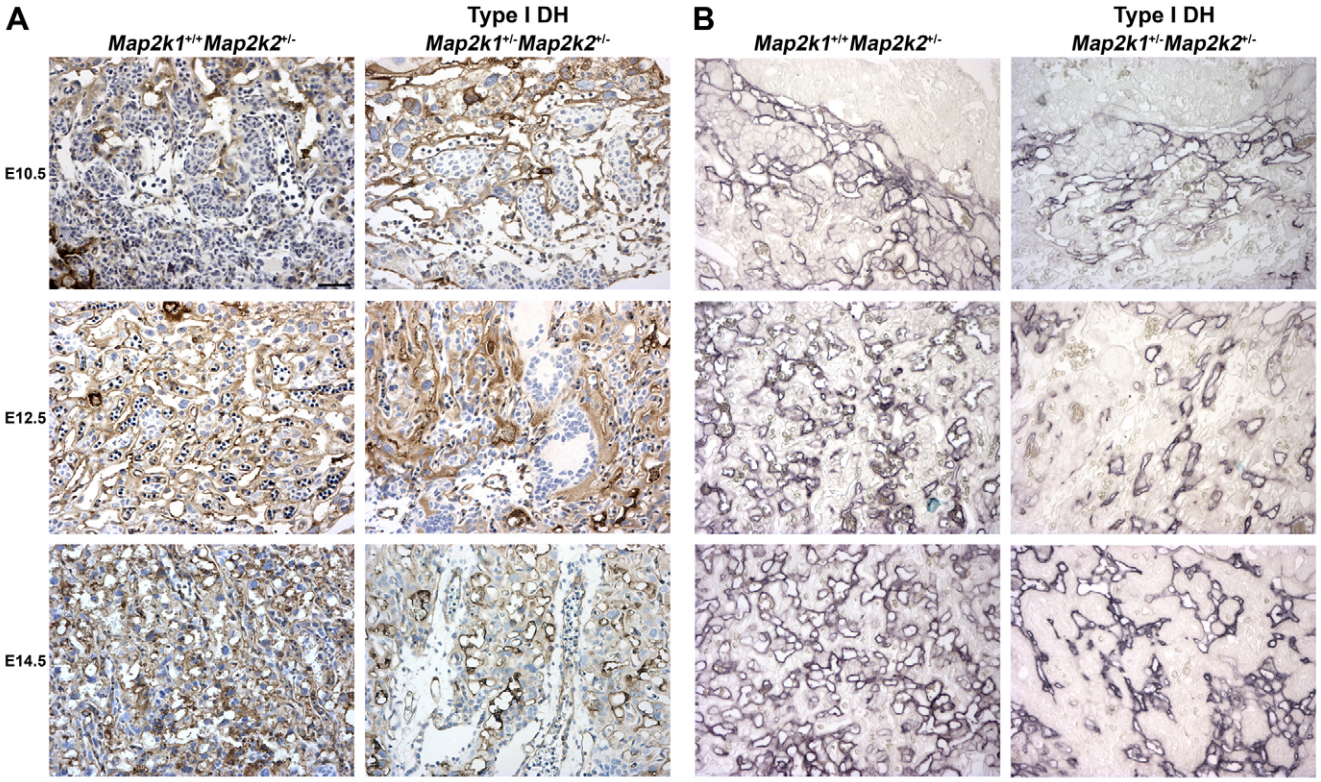

Fig. 3. Abnormal vascularization of *Map2k1*$^{+/-}$*Map2k2*$^{+/-}$ placenta labyrinth. (**A**) The embryonic vascular network of E10.5, E12.5 and E14.5 control (*Map2k1*$^{+/+}$*Map2k2*$^{+/-}$) and type I DH placentas was revealed by anti-CD31 staining. (**B**) The maternal sinuses were detected using alkaline phosphatase activity, which labels the cells lining the maternal blood network. In type I DH placentas (*Map2k1*$^{+/-}$*Map2k2*$^{+/-}$), the fetal blood vessels as well as the maternal sinuses were less abundant when compared with the control specimens at all stages analyzed. Scale bar: 50 μm.

2002). This specific breeding should provide all the genotypes required for control and experimental specimens. The *Map2k1*$^{+/flox}$*Map2k2*$^{+/-}$*Tg*$^{+/+}$ progeny was used to define the normal survival rate whereas the *Map2k1*$^{+/\Delta}$*Map2k2*$^{+/-}$*Tg*$^{+/+}$ and *Map2k1*$^{+/\Delta}$*Map2k2*$^{+/-}$*Tg*$^{+/Sox2Cre}$ specimens monitored DH defective survival. Finally, the *Map2k1*$^{+/flox}$*Map2k2*$^{+/-}$*Tg*$^{+/Sox2Cre}$ conceptuses addressed the contribution of extra-embryonic development to DH survival. In the latter case, genotype of the embryo differed from that of the extra-embryonic tissues: the embryo was *Map2k1*$^{+/\Delta}$*Map2k2*$^{+/-}$ whereas the extra-embryonic structures were *Map2k1*$^{+/flox}$*Map2k2*$^{+/-}$. As expected, the survival rate at weaning of *Map2k1*$^{+/\Delta}$*Map2k2*$^{+/-}$*Tg*$^{+/+}$ mutants was reduced compared with that of *Map2k1*$^{+/flox}$*Map2k2*$^{+/-}$*Tg*$^{+/+}$ mice (8% instead of 25%, $P<0.0001$) (Table 2). However, *Map2k1*$^{+/\Delta}$*Map2k2*$^{+/-}$*Tg*$^{+/Sox2Cre}$ and *Map2k1*$^{+/flox}$*Map2k2*$^{+/-}$*Tg*$^{+/Sox2Cre}$ mice could not be distinguished by genotyping, but together they were represented at the expected Mendelian ratio (Table 2). To distinguish the *Map2k1*$^{+/\Delta}$*Map2k2*$^{+/-}$*Tg*$^{+/Sox2Cre}$ and *Map2k1*$^{+/flox}$*Map2k2*$^{+/-}$*Tg*$^{+/Sox2Cre}$ specimens, litters were recovered at E18.5 to allow genotyping of extra-embryonic tissues (Table 2). The genotypes of the embryos and their yolk sacs were independently determined. The number of embryos obtained for each genotype diverged significantly from the expected ratio ($P<0.018$). The number of *Map2k1*$^{+/\Delta}$*Map2k2*$^{+/-}$*Tg*$^{+/+}$ and *Map2k1*$^{+/\Delta}$*Map2k2*$^{+/-}$*Tg*$^{+/Sox2Cre}$ embryos was reduced when compared with that of *Map2k1*$^{+/flox}$*Map2k2*$^{+/-}$*Tg*$^{+/+}$ controls. Most importantly, restriction of haploinsufficiency to the embryo in *Map2k1*$^{+/flox}$*Map2k2*$^{+/-}$*Tg*$^{+/Sox2Cre}$ specimens had no impact on survival rate. Thus, the rescue of the placenta phenotype allows the normal development of DH embryos and establishes that *Map2k1* and *Map2k2* gene dosage is crucial for extra-embryonic structure formation.

Unequal gene dosage-dependent contribution of *Map2k1* and *Map2k2* to placenta development

The lack of phenotype in *Map2k2* homozygous mutant mice contrasts with the lethality of the *Map2k1*$^{+/-}$*Map2k2*$^{+/-}$ embryos. The *Map2k2* mutation participates in the lethal phenotype only in the absence of one *Map2k1* allele, suggesting a gene dosage effect in which *Map2k1* and *Map2k2* genes do not contribute equally to the development of the extra-embryonic structures. To define the share of each gene in placenta development, *Map2k1*$^{+/-}$*Map2k2*$^{+/-}$ mutant mice were intercrossed and their progenies analyzed. As the number of *Map2k1*$^{+/-}$*Map2k2*$^{+/-}$ mice obtained by *Map2k2*$^{-/-}$ × *Map2k1*$^{+/-}$ breeding was limiting, we also performed *Map2k1*$^{flox/flox}$ × *Map2k2*$^{-/-}$*Tg*$^{+/Sox2Cre}$ breedings to generate *Map2k1*$^{+/\Delta}$*Map2k2*$^{+/-}$ mice. The *Map2k1* deletion restricted to the embryo allowed the complete survival of *Map2k1*$^{+/\Delta}$*Map2k2*$^{+/-}$ mutants. DH intercrosses, using either *Map2k1*$^{+/}$ *Map2k2*$^{+/-}$ or *Map2k1*$^{+/\Delta}$*Map2k2*$^{+/-}$ mice, generated similar results (Table 3A,B). Analysis of the genotype distribution at weaning revealed that the deletion of both *Map2k1* alleles led to embryonic death whereas the lethality associated with the homozygous *Map2k2* mutation required the absence of at least one *Map2k1* allele. To establish at which embryonic age *Map2k1Map2k2* compound mutants die, the analysis was also performed at E10.5 (Table 3). Most of the allelic combinations were obtained at the expected

Table 2. Rescue of *Map2k1*$^{+/-}$*Map2k2*$^{+/-}$ embryos with a specific *Map2k1* deletion in embryonic tissues

Map2k1$^{flox/\Delta}$*Map2k2*$^{+/+}$×*Map2k1*$^{+/+}$*Map2k2*$^{-/-}$*Tg*$^{+/Sox2Cre}$

				Genotype of live embryos			
				Tg$^{+/Sox2Cre}$		*Tg*$^{+/+}$	
Age	Number of litters	Number of pups	Genotype of extra-embryonic structure: / Genotype of embryo:	*Map2k1*$^{+/flox}$*Map2k2*$^{+/-}$ / *Map2k1*$^{+/\Delta}$*Map2k2*$^{+/-}$	*Map2k1*$^{+/\Delta}$*Map2k2*$^{+/-}$ / *Map2k1*$^{+/\Delta}$*Map2k2*$^{+/-}$	*Map2k1*$^{+/flox}$*Map2k2*$^{+/-}$ / *Map2k1*$^{+/flox}$*Map2k2*$^{+/-}$	*Map2k1*$^{+/\Delta}$*Map2k2*$^{+/-}$ / *Map2k1*$^{+/\Delta}$*Map2k2*$^{+/-}$
E18.5	17	90		33 (37%)	17 (19%)	25 (28%)	15 (17%)
W3-4	11	48		26 (54%)*		18 (38%)	4 (8%)
Expected %				25%	25%	25%	25%

*The genotype of the extra-embryonic tissues could not be determined.

Mendelian ratio except for the *Map2k1*$^{-/-}$*Map2k2*$^{+/-}$ and *Map2k1*$^{-/-}$*Map2k2*$^{-/-}$ genotypes, indicating an earlier embryonic death. Histology of E10.5 placentas carrying the allelic combinations recovered showed a gradation in the severity of the phenotype (Fig. 4). Normal development of the labyrinth region was observed in *Map2k1*$^{+/+}$*Map2k2*$^{+/-}$, *Map2k1*$^{+/+}$*Map2k2*$^{-/-}$ and *Map2k1*$^{+/\Delta}$*Map2k2*$^{+/+}$ specimens when compared to wild-type controls (Fig. 4A-D). Some *Map2k1*$^{+/\Delta}$*Map2k2*$^{+/-}$ mutants displayed a normal phenotype (type II DH mutants) (Fig. 4E), whereas others presented placenta defects (type I DH mutants) as previously shown (Fig. 1). All *Map2k1*$^{\Delta/+}$*Map2k2*$^{-/-}$ specimens presented a more severe phenotype with an increased reduction of the labyrinth region and the presence of MTG cells (Fig. 4F). The most severe placenta phenotype was detected in *Map2k1*$^{\Delta/\Delta}$*Map2k2*$^{+/+}$ and *Map2k1*$^{\Delta/\Delta}$*Map2k2*$^{+/-}$ specimens, with a very thin labyrinth region. In addition, *Map2k1*$^{\Delta/\Delta}$*Map2k2*$^{+/-}$ embryos were moribund and in the process of being resorbed. Thus, the severity of the placenta phenotype increases with the number of *Map2k* mutant alleles, demonstrating that the correct development of extra-embryonic structures requires a proper *Map2k* gene dosage.

To determine whether the placenta defect was responsible for the reduced survival rate of the *Map2k1*$^{+/\Delta}$*Map2k2*$^{-/-}$ conceptuses, we performed rescue of the placenta phenotype to determine whether *Map2k1*$^{+/\Delta}$*Map2k2*$^{-/-}$ mice can survive to adulthood. When *Map2k1*$^{flox/flox}$*Map2k2*$^{-/-}$ females were bred with *Map2k1*$^{+/+}$*Map2k2*$^{-/-}$*Tg*$^{+/Sox2Cre}$ males, the expected Mendelian ratio of *Map2k1*$^{+/\Delta}$*Map2k2*$^{-/-}$ animals was recovered (12 over 22 pups born) indicating that only one *Map2k1* allele is sufficient for normal embryo development in the absence of *Map2k2* gene function when the placenta can develop normally.

The gene dosage-dependent placenta defects correlate with a decrease in ERK/MAPK activation

To determine if the gene dosage-dependent defects of placenta development were due to perturbed ERK/MAPK signaling, we performed western blot analyses with embryo and placenta whole protein extracts from E10.5 wild-type and *Map2k1Map2k2* compound mutants using a phospho-specific MAPK1/MAPK3 antibody (Fig. 5A). To do so, *Map2k1*$^{+/\Delta}$*Map2k2*$^{+/-}$ mice were intercrossed and the conceptuses were used for protein extraction. The phosphorylation of MAPKs at specific residues of the activation loop is usually a good read-out of their state of activation (Gopalbhai et al., 2003). MAP2K1 and MAP2K2 protein levels were also evaluated. Signal for MAP2K1 and MAP2K2 was sometimes detected in placenta samples from homozygous null mutants, indicating cross-contamination with maternal tissues. The reduction in phosphorylation of MAPK1 and MAPK3 was the most severe in *Map2k1*$^{\Delta/\Delta}$*Map2k2*$^{+/+}$ and *Map2k1*$^{+/\Delta}$*Map2k2*$^{-/-}$ placenta and embryonic samples. A likely explanation for this decrease could be that *Map2k1*$^{\Delta/\Delta}$*Map2k2*$^{+/+}$ and *Map2k1*$^{+/\Delta}$*Map2k2*$^{-/-}$ embryos were dying and in the process of resorption. In this experiment, no *Map2k1*$^{-/-}$*Map2k2*$^{+/-}$ specimen was obtained. Together, these results support the

Table 3. Gradation of the placental phenotype in function of the number of *Map2k* mutant alleles

(A) *Map2k1*$^{+/-}$*Map2k2*$^{+/-}$×*Map2k1*$^{+/-}$*Map2k2*$^{+/-}$

		Genotype of live embryos or mice								
Age	Number of pups	*Map2k1*$^{+/+}$ *Map2k2*$^{+/+}$	*Map2k1*$^{+/+}$ *Map2k2*$^{+/-}$	*Map2k1*$^{+/+}$ *Map2k2*$^{-/-}$	*Map2k1*$^{+/-}$ *Map2k2*$^{+/+}$	*Map2k1*$^{+/-}$ *Map2k2*$^{+/-}$	*Map2k1*$^{+/-}$ *Map2k2*$^{-/-}$	*Map2k1*$^{-/-}$ *Map2k2*$^{+/+}$	*Map2k1*$^{-/-}$ *Map2k2*$^{+/-}$	*Map2k1*$^{-/-}$ *Map2k2*$^{-/-}$
E10.5	30	2 (6.7%)	2 (6.7%)	3 (10.0%)	3 (10.0%)	8 (26.7%)	6 (20.0%)	6 (20.0%)	0 (0%)	0 (0%)
W3-4	15	1 (6.7%)	6 (40%)	2 (13.3%)	3 (20%)	3 (20%)	0 (0%)	0 (0%)	0 (0%)	0 (0%)
Expected %		6.25%	12.5%	6.25%	12.5%	25%	12.5%	6.25%	12.5%	6.25%

(B) *Map2k1*$^{+/\Delta}$*Map2k2*$^{+/-}$×*Map2k1*$^{+/\Delta}$*Map2k2*$^{+/-}$

		Genotype of live embryos or mice								
Age	Number of pups	*Map2k1*$^{+/+}$ *Map2k2*$^{+/+}$	*Map2k1*$^{+/+}$ *Map2k2*$^{+/-}$	*Map2k1*$^{+/+}$ *Map2k2*$^{-/-}$	*Map2k1*$^{+/\Delta}$ *Map2k2*$^{+/+}$	*Map2k1*$^{+/\Delta}$ *Map2k2*$^{+/-}$	*Map2k1*$^{+/\Delta}$ *Map2k2*$^{-/-}$	*Map2k1*$^{\Delta/\Delta}$ *Map2k2*$^{+/+}$	*Map2k1*$^{\Delta/\Delta}$ *Map2k2*$^{+/-}$	*Map2k1*$^{\Delta/\Delta}$ *Map2k2*$^{-/-}$
E10.5	87	2 (2.3%)	12 (13.8%)	6 (6.9%)	17 (19.5%)	28 (32.2%)	11 (12.6%)	8 (9.2%)	3 (3.4%)	0 (0%)
W3-4	11	1 (9.1%)	1 (9.1%)	1 (9.1%)	4 (36.3%)	4 (36.3%)	0 (0%)	0 (0%)	0 (0%)	0 (0%)
Expected %		6.25%	12.5%	6.25%	12.5%	25%	12.5%	6.25%	12.5%	6.25%

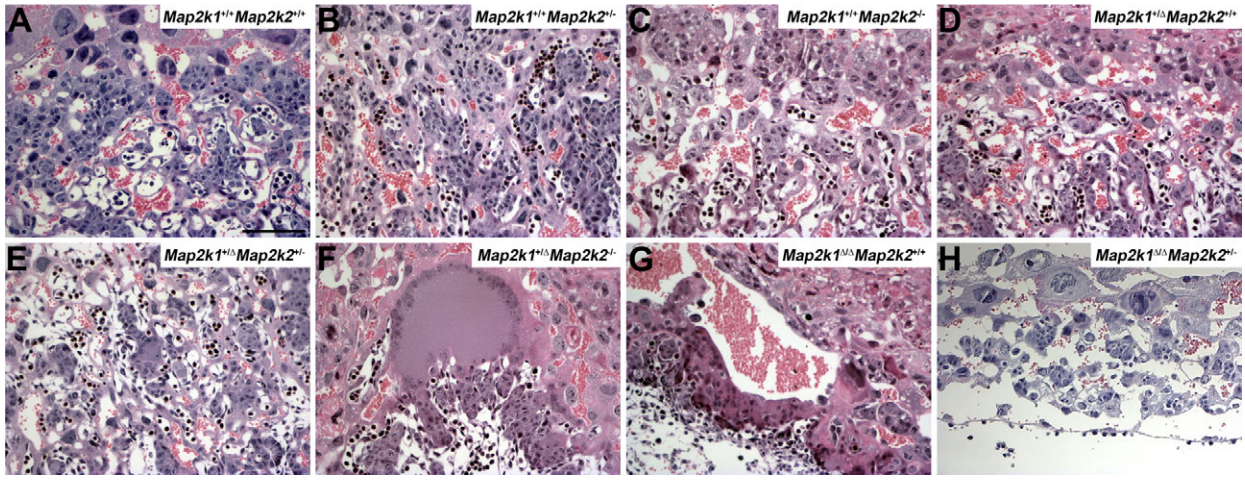

Fig. 4. Placenta phenotype of *Map2k1Map2k2* compound mutants. Hematoxylin and Eosin staining of E10.5 placenta sections from embryos carrying all possible allelic combinations except the *Map2k1*$^{-/-}$*Map2k2*$^{-/-}$ mutants that were never obtained. (**A-D**) *Map2k1 Map2k2* genotypes that conferred a normal labyrinth development. (**E-H**) Compound mutants exhibiting placenta defects, the severity of which increases as seen from left to right. The most severe phenotype was observed in *Map2k1*$^{\Delta/\Delta}$*Map2k2*$^{+/-}$ specimens (H). Scale bar: 100 μm.

correlation between the gene dosage-dependent placenta defect, the reduction of the ERK/MAPK signaling and the predominant role of *Map2k1*.

We have previously shown that the ERK/MAPK cascade is highly activated in the SynT of the labyrinth and that this activation is lost in *Map2k1*$^{-/-}$ specimens (Bissonauth et al., 2006). To correlate ERK/MAPK cascade activation with the specific expression of either MAP2K1 or MAP2K2 proteins, the expression profile of the MAP2K1 and MAP2K2 proteins was established by immunohistochemistry (Fig. 5B). The specificity of the antibodies was demonstrated on *Map2k1*$^{-/-}$ and *Map2k2*$^{-/-}$ placenta sections, and as expected no MAP2K1 and MAP2K2 proteins were detected on sections of *Map2k1*$^{-/-}$ and *Map2k2*$^{-/-}$ specimens, respectively. The expression of the MAP2K2 protein was ubiquitous in the placenta. By contrast, the MAP2K1 protein was strongly detected in cells lining the maternal sinuses (Fig. 5B, arrow), but not in mononuclear giant cells (Fig. 5B, arrowheads).

Aberrant formation of multinucleated trophoblast giant cells derived from the SynT layer II

The formation of MTG cells in specimens lacking one or both *Map2k2* alleles in *Map2k1*$^{+/-}$ conceptuses was an unusual *Map2k2*-dependent phenotype (Fig. 1; Fig. 4F). These MTG cells were

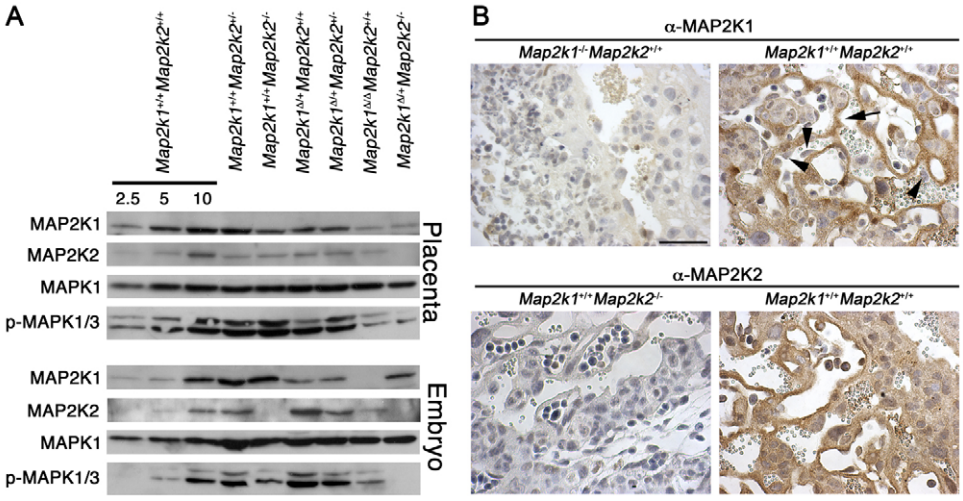

Fig. 5. ERK/MAPK activation in *Map2k1Map2k2* compound mutants and differential expression of MAP2K1 and MAP2K2 proteins in the placenta. (**A**) Expression of MAPK1, MAP2K1 and MAP2K2 proteins, and phosphorylation levels of MAPK1/MAPK3 were evaluated by western blot analysis of total protein extracts from E.10.5 wild-type and *Map2k1Map2k2* compound mutant placentas and embryos. The analyses of embryonic and placenta extracts from compound mutants without *Map2k1* or *Map2k2* gene function revealed that the placenta could be contaminated by maternal tissues during dissection, as traces of MAP2K1 or MAP2K2 proteins were observed in few samples. Phosphorylation of MAPK1 and MAPK3 was significantly reduced in *Map2k1*$^{\Delta/\Delta}$*Map2k2*$^{+/+}$ and *Map2k1*$^{+/\Delta}$*Map2k2*$^{-/-}$ embryos and placentas. MAPK1 detection was used as loading control. (**B**) MAP2K1 and MAP2K2 immunostaining was performed on E10.5 wild-type, *Map2k1*$^{-/-}$ and *Map2k2*$^{-/-}$ placentas. Controls were done without primary antibody (not shown), and the specificity of each antibody was confirmed on *Map2k1*$^{-/-}$ or *Map2k2*$^{-/-}$ specimens. In wild-type specimens, MAP2K1 was mainly detected in the cells lining the maternal sinuses most likely the SynT (arrow) and no expression was detected in the mononuclear giant cells (arrowheads). MAP2K2 expression was ubiquitous in the placenta. Scale bar: 50 μm.

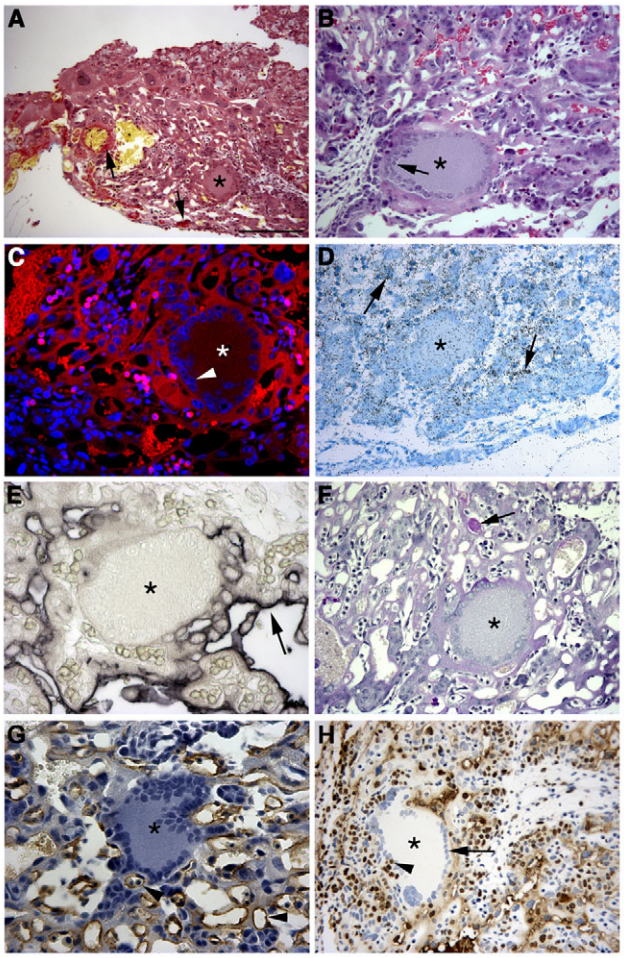

Fig. 6. Characterization of the MTG cells in *Map2k1*$^{+/-}$*Map2k2*$^{+/-}$ placentas. (**A**) In E12.5 type I DH mutant placenta sections, the MTG cells, indicated by an asterisk, were devoid of fibrin deposits stained in red with MSB (arrows). (**B**) Hematoxylin and Eosin staining showed the presence of MTG cells with multiple nuclei located at the periphery (arrow). (**C**) The multinucleated nature of the MTG cells was also revealed by the DAPI/Phalloidin staining (arrowhead). The absence of *Gcm1* expression (**D**) and alkaline phosphatase activity (**E**) in MTG cells suggested that they were not SynT. The arrows indicate positive signals. (**F**) No PAS staining was detected in MTG cells, indicating that they were not glycogen trophoblast cells (arrow). (**G**) The MTG cells were also negative for CD31, indicating that they were not vascular endothelial cells (arrowhead). (**H**) No BrdU incorporation in the nuclei of the MTG cells (arrow) was observed, indicating that these cells are post-mitotic as the SynT. Positive nuclei adjacent to the nuclei of the MTG cells were rarely observed (arrowhead). Scale bars: 200 μm in A; 100 μm in B,C,D,F,H; 50 μm in E,G.

observed as early as E10.5 in more than 50% of the *Map2k1*$^{+/-}$*Map2k2*$^{+/-}$ specimens analyzed (three out of five). Even if they were not strictly associated with type I DH mutants, their number was more abundant in this type. MTG were observed throughout the labyrinth and restricted to this layer. The number and the size of MTG was greater in type I DH mutants, and they increased at E12.5 and decreased at E14.5, most likely because the most affected specimens died between these two ages (Table 4). The presence of the MTG cells suggested an aberrant SynT differentiation, which can contribute to the reduced vascularization of the placenta due to impaired branching morphogenesis (Fig. 3) (Bissonauth et al., 2006). A similar structure was previously reported in *Lbp-1a* mutants and referred to 'amorphous material' (Parekh et al., 2004). It was suggested to represent fibrin deposits derived from extravasation of blood from a defective vascular bed. To reveal any fibrin deposit in our specimens, we performed MSB staining. Even though MSB staining was observed in wild-type and *Map2k1*$^{+/-}$*Map2k2*$^{+/-}$ placentas, the MTG cells were negative (Fig. 6A). Hematoxylin and Eosin staining clearly showed the multinucleated nature of these structures, with the nuclei located at the periphery (Fig. 6B). This result was corroborated by staining the nuclei with DAPI and the cortical actin with phalloidin (Fig. 6C). The actin signal was restricted to the periphery of the MTG cells with the juxtaposed nuclei. No phalloidin staining was observed between the nuclei in the multinucleated cells, suggesting the absence of cytoplasmic membrane. Altogether, these results indicate that these structures are multinucleated cells devoid of fibrin deposits.

As the multinucleated cell type of the placenta is the SynT, we wanted to establish whether MTG cells were SynT-derived using specific markers such as alkaline phosphatase activity for the SynT and *Gcm1* expression for the SynT layer II (SynT-II) (Simmons et al., 2008). *Gcm1*-positive cells were detected in *Map2k1*$^{+/-}$*Map2k2*$^{+/-}$ labyrinth (Fig. 6D), but the MTG cells were negative for *Gcm1* expression. Similarly, alkaline phosphatase activity was detected in cells lining the maternal sinuses but not in MTG cells (Fig. 6E). MTG cells were negative for other cell lineage markers such as the glycogen trophoblasts detected by PAS staining (Fig. 6F) and the spongiotrophoblasts (detected by in situ hybridization using *Tpbpa*; not shown). The MTG cells were also negative for CD31, indicating that they were not vascular endothelial cells (Fig. 6G). Finally, the MTG cells were negative for BrdU incorporation, indicating that they were post-mitotic cells like the SynT (Fig. 6H) (Cross et al., 2006).

Table 4. Characterization of the MTG in *Map2k1*$^{+/-}$*Map2k2*$^{+/-}$ placentas

Age	Type of DH mutant	Number of specimens with MTG*	Average number of MTG per specimen†	Surface occupied by MTG‡ ($\times 10^{-3}$ mm^2)
E10.5	I	3/3	5.33±1.15	23.48±4.02
	II	0/2	0	NA
E12.5	I	17/17	8.71±6.46	70.25±32.50
	II	3/3	1.66±0.58	3.61±1.26
E14.5	I	5/5	6.40±3.21	23.47±7.63
	II	2/2	1.5±0.71	7.27±7.59

*The number of specimens with MTG over the total number of specimens analyzed.
†Four sections ~100 μm apart were analyzed for each specimen to estimate the number of MTG.
‡The total surface of the MTG observed in the four sections analyzed was used as an estimate.
NA, not applicable.

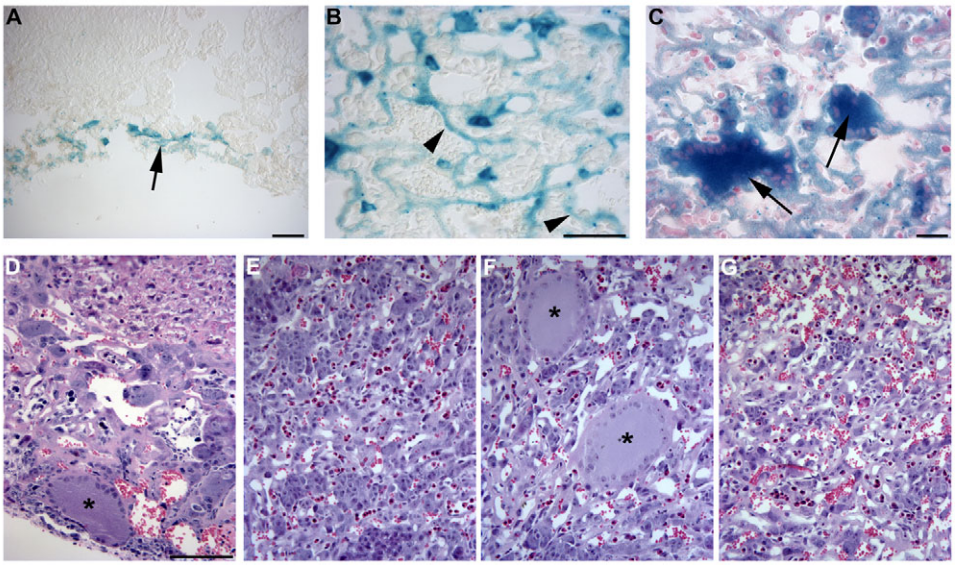

Fig. 7. The MTG cells derive from *Gcm1*-positive SynT and result from a cell-autonomous defect. (**A-C**) *lacZ* expression following *Gcm1Cre* expression in *R26R* Cre reporter mouse line. Sagittal cryosections of *Gt(ROSA)26*Sor$^{+/tm1Sor}$*Tg*$^{+/Gcm1Cre}$ placentas at E8.5 (A) and E10.5 (B) were tested for β-galactosidase activity. (A) At E8.5, *lacZ* expression was restricted to cells at the chorioallantoic interface (arrow). (B) At E10.5, the staining was limited to the cells lining the maternal sinuses (arrowheads). (C) β-galactosidase activity in *Map2k1*$^{+/\Delta}$*Map2k2*$^{+/-}$*Gt(ROSA)26*Sor$^{+/tm1Sor}$*Tg*$^{+/Gcm1Cre}$ placentas was detected in MTG cells (arrows). (**D-G**) Hematoxylin and Eosin staining of placenta sections from E12.5 *Map2k1*$^{+/-}$*Map2k2*$^{+/-}$ (D), *Map2k1*$^{+/flox}$*Map2k2*$^{+/-}$*Tg*$^{+/+}$ (E), *Map2k1*$^{+/flox}$*Map2k2*$^{+/-}$*Tg*$^{+/Gcm1Cre}$ (F) and *Map2k1*$^{+/flox}$*Map2k2*$^{+/-}$*Tg*$^{+/Sox2Cre}$ (G) specimens. (D) MTG cells indicated by the asterisk were detected in *Map2k1*$^{+/-}$*Map2k2*$^{+/-}$ positive control. The specific inactivation of one *Map2k1* allele in *Map2k2*$^{+/-}$ SynT-II (*Map2k1*$^{+/flox}$*Map2k2*$^{+/-}$*Tg*$^{+/Gcm1Cre}$) led to the formation of MTG cells (F). By contrast, when the *Map2k1* deletion was restricted to the embryo (*Map2k1*$^{+/flox}$*Map2k2*$^{+/-}$*Tg*$^{+/Sox2Cre}$), no MTG cells were observed in placenta (G). Scale bars: 50 μm in A; 100 μm in B-G.

Few BrdU-positive nuclei were found adjacent to the nuclei of the MTG cells but it was difficult to assess if they were part of the MTG cells or not (Fig. 6H). Thus, the formation of the MTG did not seem to be due to defective cytokinesis.

To further investigate the origin of the MTG cells, we used a genetic-based approach to follow the *Gcm1*-expressing SynT-II cell lineage. A *Gcm1Cre* transgenic mouse line expressing the Cre recombinase in the SynT-II cells was produced and characterized by breeding to the *R26R* Cre reporter mouse line for monitoring Cre expression (*Gt(ROSA)26*Sor^{tm1Sor} allele) (Soriano, 1999). At E8.5, *Gt(ROSA)26*Sor$^{+/tm1Sor}$*Tg*$^{+/Gcm1Cre}$ placentas displayed X-Gal staining restricted to the chorionic cells, whereas at E10.5 staining was restricted to the cells lining the maternal sinuses (Fig. 7A,B). This reproduced the placenta *lacZ* expression profile previously described in *Gcm1-lacZ* knock-in mice as well as the expression pattern of the endogenous *Gcm1* gene (Basyuk et al., 1999; Schreiber et al., 2000; Stecca et al., 2002). We thus used the *Gcm1Cre* mice to determine if the MTG cells were derived from the SynT-II cells. *Map2k1*$^{+/\Delta}$*Tg*$^{+/Gcm1Cre}$ mice were mated to *Gt(ROSA)26*Sor$^{tm1Sor/tm1Sor}$*Map2k2*$^{-/-}$ mice and E12.5 progenies were analyzed for the presence of MTG cells. The latter were detected in *Map2k1*$^{+/\Delta}$*Map2k2*$^{+/-}$*Gt(ROSA)26*Sor$^{+/tm1Sor}$*Tg*$^{+/Gcm1Cre}$ and *Map2k1*$^{+/\Delta}$*Map2k2*$^{+/-}$*Gt(ROSA)26*Sor$^{+/tm1Sor}$*Tg*$^{+/+}$ specimens. However, the structures were positive for X-Gal staining only when positive for the *Gcm1Cre* transgene, indicating that the MTG cells derived from SynT-II (Fig. 7C).

The formation of MTG cells is a cell-autonomous defect

In *Lbp-1a* null mutants, the presence of multinucleated cells in the placenta cannot be rescued in tetraploid complementation assays, indicating that the defect is non-cell-autonomous (Parekh et al., 2004). The placenta phenotype in *Lbp-1a*$^{-/-}$ embryos is secondary to a defective allantoic mesoderm. LBP-1 protein isoforms are phosphorylated by the ERK/MAPK cascade and their phosphorylation might affect their cellular localization as well as their DNA-binding activity (Pagon et al., 2003; Sato et al., 2005; Volker et al., 1997). We tested if the accumulation of MTG cells in *Map2k1*$^{+/-}$*Map2k2*$^{+/-}$ was a cell-autonomous defect or not. *Map2k1*$^{flox/flox}$*Map2k2*$^{-/-}$ females were first bred with *Tg*$^{+/Gcm1Cre}$ males to restrict the *Map2k1* deletion to the SynT-II cells (Fig. 7D-F). The specific deletion of one *Map2k1* allele in SynT-II from the *Map2k1*$^{+/flox}$*Map2k2*$^{+/-}$*Tg*$^{+/Gcm1Cre}$ conceptuses led to formation of MTG cells, as detected in placentas from three E12.5 specimens analyzed (Fig. 7F). By contrast, the placenta from *Map2k1*$^{+/flox}$*Map2k2*$^{+/-}$*Tg*$^{+/Sox2Cre}$ specimens did not include any MTG structure (seven specimens analyzed) (Fig. 7G). The complete deletion of the *Map2k1*^{flox} allele in embryonic tissues by *Sox2Cre* was confirmed by genotyping analyses (Fig. S3 in the supplementary material). Thus, the formation of MTG cells required the deletion of one allele of each *Map2k1* and *Map2k2* genes in the SynT-II, indicating that the phenotype is cell-autonomous. However, as the *Map2k2* mutation is not restricted to the SynT-II, we cannot rule out a potential contribution of MAP2K2 in endothelial cells to the MTG phenotype.

The MTG are derived from SynT-II cells and the ERK/MAPK cascade is highly activated in SynT-II, leading us to investigate the ERK/MAPK activation in MTG. Both MAP2K1 and MAP2K2 were expressed in SynT-II-derived MTG, as assessed by immunohistochemistry (Fig. 8B,D). They were also activated in MTG, as seen with an anti-phospho-MAP2K1/2 (Fig. 8F). However, no phospho-MAPK1/3 staining was detected in MTG, revealing the absence of ERK/MAPK activation (Fig. 8H). These data indicate that the sustained activation of the ERK/MAPK cascade is required for the formation of the uniform SynT layer II lining the maternal sinuses.

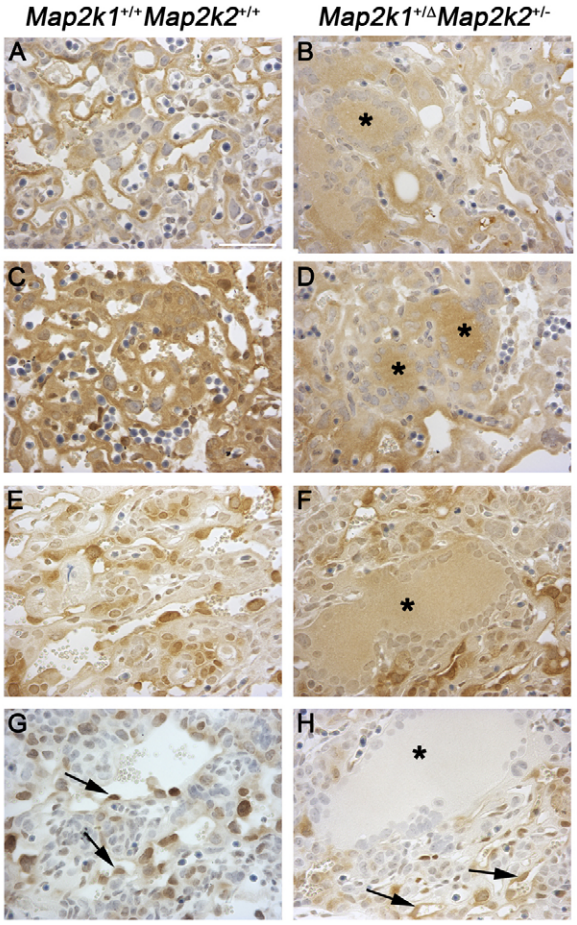

Fig. 8. Lack of MAPK1 and MAPK3 activation in MTG cells. MAP2K1 (**A**,**B**), MAP2K2 (**C**,**D**), phospho-MAP2K1/2 (**E**,**F**) and phospho-MAPK1/3 (**G**,**H**) immunostainings were performed on E12.5 wild-type (A,C,E,G) and *Map2k1*$^{+/\Delta}$*Map2k2*$^{+/-}$ (B,D,F,H) placentas. MAP2K1, MAP2K2 and phospho-MAP2K1/2 were detected in MTG (*) cells. Phospho-MAPK1/3 was detected in SynT lining the maternal sinuses (arrows) from wild-type (G) and *Map2k1*$^{+/\Delta}$*Map2k2*$^{+/-}$ (H) specimens but not in the MTG. Scale bar: 50 μm.

DISCUSSION

The disruption of the murine *Map2k1* gene leads to an embryonic lethal phenotype caused by the underdevelopment of the placenta labyrinth associated with its hypovascularization, revealing the essential role of *Map2k1* in extra-embryonic development (Bissonauth et al., 2006; Giroux et al., 1999). By contrast, the absence of phenotype in *Map2k2* mutants suggests that *Map2k2* is dispensable as *Map2k1* can compensate for the lack of *Map2k2* gene function (Bélanger et al., 2003). We have previously shown that both *Map2k1* and *Map2k2* genes are widely expressed in the embryo and the placenta (Bissonauth et al., 2006; Giroux et al., 1999). In this study, we asked whether haploinsufficiency of the *Map2k1* locus could reveal *Map2k2* gene function during mouse development. Our data clearly show that the lack of one or both *Map2k2* alleles in *Map2k1*$^{+/-}$ mice causes embryonic death consistent with a role of *Map2k2* in embryonic development. *Map2k1*$^{+/-}$*Map2k2*$^{+/-}$ mice have a reduced survival rate whereas the *Map2k1*$^{+/-}$ *Map2k2*$^{-/-}$ embryos die at early gestation if *Map2k1* is deleted in both embryonic and extra-embryonic tissues (Tables 1 and 3). However, when the deletion of *Map2k1* is restricted to embryonic tissues, *Map2k1*$^{+/\Delta}$*Map2k2*$^{+/-}$ and *Map2k1*$^{+/\Delta}$*Map2k2*$^{-/-}$ mice are viable and represented at weaning according to the Mendelian distribution. These results indicate that both *Map2k1* and *Map2k2* genes contribute to the development of the extra-embryonic ectoderm whereas only one allele of *Map2k1* is sufficient for embryo development and signaling in adult mice. It would be interesting to determine if a similar result is obtained when only one *Map2k2* functional allele is retained in adult.

Gene duplication is a common event and has led to the production of numerous gene families in multiple species, including mammals. During evolution, two highly conserved *Map2k* genes, *Map2k1* and *Map2k2*, have arisen from a single prototypic gene as a result of genome duplication. Following gene duplication, decreased selection pressure can sometimes allow production of proteins with novel function or expression profile resulting in partial redundancy among gene family members. The biochemical properties of MAP2K1 and MAP2K2 proteins suggest that these two enzymes have evolved to be differentially utilized (Skarpen et al., 2007; Ussar and Voss, 2004). If the shared function of duplicated genes becomes unequally distributed between gene copies, unequal redundancy among the gene family members may result, as observed for the *Erk/Map2k* gene family, where the *Map2k2* gene deletion does not cause any phenotype but enhances the *Map2k1* placenta defects in a unique manner. Our study uncovers unequal contribution and gene dosage effect of the *Erk/Map2k* genes that exhibit overlapping expression profile (Fig. 5) (Bissonauth et al., 2006; Giroux et al., 1999). *Map2k2*$^{-/-}$ mutants show no obvious defect in placenta and embryo development, indicating that *Map2k1* expression is sufficient and above the MAP2K threshold levels essential for correct placenta development. As successive *Map2k* alleles are mutated, MAP2K1 and MAP2K2 levels became inadequate to maintain signaling and placenta defects occur.

The reduction of trophoblast proliferation and the hypovascularization of the labyrinth region, which both characterize the *Map2k1*$^{-/-}$ placenta phenotype, were also observed in *Map2k1*$^{+/-}$*Map2k2*$^{+/-}$ specimens. The contribution of *Map2k1* to the phenotype appears predominant over that of *Map2k2*. Consistent with this unequal gene dosage-dependent model, the severity of the placenta phenotype increases with the number of *Map2k* null alleles: *Map2k1*$^{+/-}$*Map2k2*$^{+/-}$<*Map2k1*$^{+/-}$*Map2k2*$^{-/-}$<*Map2k1*$^{-/-}$*Map2k2*$^{+/+}$ <*Map2k1*$^{-/-}$*Map2k2*$^{+/-}$, the *Map2k1*$^{-/-}$*Map2k2*$^{+/-}$ placentas presenting the most severe phenotype. Moreover, this is paralleled by a gradation in ERK/MAPK activation (Fig. 5A).

In many cases, unequal redundancy between paralogs may be produced by differences in expression levels, distinct expression profiles or acquisition of new protein functions. Previous studies have shown that both MAP2K1 and MAP2K2 proteins are expressed at similar levels in several cell lines. However, in some cell lines MAP2K1 is present in slight excess (Xu et al., 1997). Furthermore, MAP2K2 has been shown to be the most active ERK activator (Zheng and Guan, 1993). Recombinant MAP2K1 has an activity approximately seven times lower than that of MAP2K2. However, this difference in activity does not take into account the presence in cells of various mechanisms that can increase the specificity and the enzymatic activity of MAP2K proteins. For instance, the MAP2K1 interacting protein 1 (MAP2K1ip1), a scaffolding protein, has been shown to enhance the enzymatic activity of MAP2K1 towards MAPK1 and MAPK3, to interfere with feedback inhibition of MAP2K1 by MAPK1, and to inhibit the ability of activated MAPK1 to phosphorylate the transcription factors ETS-1 and ETS-2 (Brahma and Dalby, 2007; Foulds et al., 2004; Schaeffer et al., 1998). MAP2K2 does not form a stable

complex with MAP2K1ip1. In the placenta, both MAP2K1 and MAP2K2 proteins are co-expressed, but MAP2K1 is expressed at higher levels in the SynT (Fig. 5B). This raises the possibility that MAP2K1 enzymatic activity is more important for this cell lineage than MAP2K2 one. In absence of both *Map2k1* functional alleles, ERK activation levels may be under threshold whereas the deletion of one allele of each *Map2k* gene may not have such an impact since some DH mutants survive at birth. Thus, the different phenotypes observed might be due to variations in *Map2k* expression levels or domains. However, we cannot exclude that each MAP2K protein may possess unique properties.

The loss of *Map2k2* function when combined with *Map2k1* haploinsufficiency results in the accumulation of MTG cells in the placenta. A cell-lineage approach using the *Gcm1Cre* deleter mouse line has revealed the SynT-II origin of the MTG cells as well as the cell-autonomous nature of the defect. Even though the MAP2K1 protein is detected at high levels in SynT, no MTG cells were observed in $Map2k1^{+/-}$ and $Map2k1^{-/-}$ placentas (Fig. 4; see Fig. S2 in the supplementary material) (Bissonauth et al., 2006). Moreover, SynT-II are determined at the right time based on *Gcm1* expression in $Map2k1^{-/-}$ specimens, despite their restricted localization at the chorioallantoic interface that underlies the defective placenta vascularization (Bissonauth et al., 2006). This indicates the importance of *Map2k2* mutation in the formation of MTG cells.

The presence of MTG cells has been reported for the *Sos1* and *Lbp-1a* mouse mutants (Parekh et al., 2004; Qian et al., 2000). *Sos1* is upstream of MAP2K1 and MAP2K2 in the ERK/MAPK cascade. Moreover, in E10.5 embryo, most ERK activity was shown to be *Sos1*-dependent (Qian et al., 2000). Therefore, it is not surprising that *Sos1* and *Map2k1Map2k2* compound mutants present a common placenta phenotype. By contrast, the link between *Lbp-1a* and the ERK/MAPK cascade is more indirect as the *Lbp-1a* placenta phenotype has a non-cell-autonomous origin. Normal development of the placenta includes non-cell-autonomous mechanisms involving placenta as well as embryonic paracrine factors necessary for maintaining the basic developmental program (Cross, 2005). Therefore, it is possible that LBP-1A and the ERK/MAPK cascade may complement each other, the first one by participating to the production of such paracrine signals, and the second by allowing its transduction into the cell. However, we cannot rule out the possibility that *Map2k2* haploinsufficiency impacts on LBP-1A function in the endothelial cell whereas *Map2k1* and *Map2k2* haploinsufficiency is required in the SynT-II cells for the expression of the MTG phenotype.

The present study indicates that both *Map2k1* and *Map2k2* genes are involved in extra-embryonic ectoderm formation and morphogenesis of the labyrinth, leading to its vascularization by the syncytiotrophoblasts and the embryonic blood vessels. The placenta phenotype is *Map2k1/Map2k2* gene dosage-dependent with a predominant role of *Map2k1*. Our results also reveal a unique role for *Map2k2* in SynT II cell determination and differentiation.

We thank Drs Lucie Jeannotte and Josée Aubin for critical reading of the manuscript, and François Harel for statistical analyses. This work is supported by the Canadian Institutes of Health Research (MOP-67208 to J.C.).

Supplementary material

Supplementary material for this article is available at
http://dev.biologists.org/cgi/content/full/136/8/1363/DC1

References

Acharya, U., Mallabiabarrena, A., Acharya, J. K. and Malhotra, V. (1998). Signaling via mitogen-activated protein kinase kinase (MEK1) is required for Golgi fragmentation during mitosis. *Cell* **92**, 183-192.

Aubin, J., Déry, U., Lemieux, M., Chailler, P. and Jeannotte, L. (2002). Stomach regional specification requires Hoxa5-driven mesenchymal-epithelial signaling. *Development* **129**, 4075-4087.

Basyuk, E., Cross, J. C., Corbin, J., Nakayama, H., Hunter, P., Nait-Oumesmar, B. and Lazzarini, R. A. (1999). Murine Gcm1 gene is expressed in a subset of placental trophoblast cells. *Dev. Dyn.* **214**, 303-311.

Bélanger, L. F., Roy, S., Tremblay, M., Brott, B., Steff, A. M., Mourad, W., Hugo, P., Erikson, R. and Charron, J. (2003). Mek2 is dispensable for mouse growth and development. *Mol. Cell. Biol.* **23**, 4778-4787.

Bhunia, A. K., Han, H., Snowden, A. and Chatterjee, S. (1996). Lactosylceramide stimulates Ras-GTP loading, kinases (MEK, Raf), p44 mitogen-activated protein kinase, and c-fos expression in human aortic smooth muscle cells. *J. Biol. Chem.* **271**, 10660-10666.

Bissonauth, V., Roy, S., Gravel, M., Guillemette, S. and Charron, J. (2006). Requirement for Map2k1 (Mek1) in extra-embryonic ectoderm during placentogenesis. *Development* **133**, 3429-3440.

Brahma, A. and Dalby, K. N. (2007). Regulation of protein phosphorylation within the MKK1-ERK2 complex by MP1 and the MP1*P14 heterodimer. *Arch. Biochem. Biophys.* **460**, 85-91.

Brott, B. K., Alessandrini, A., Largaespada, D. A., Copeland, N. G., Jenkins, N. A., Crews, C. M. and Erikson, R. L. (1993). MEK2 is a kinase related to MEK1 and is differentially expressed in murine tissues. *Cell Growth Differ.* **4**, 921-929.

Brunet, A., Pages, G. and Pouyssegur, J. (1994). Growth factor-stimulated MAP kinase induces rapid retrophosphorylation and inhibition of MAP kinase kinase (MEK1). *FEBS Lett.* **346**, 299-303.

Catling, A. D., Schaeffer, H. J., Reuter, C. W., Reddy, G. R. and Weber, M. J. (1995). A proline-rich sequence unique to MEK1 and MEK2 is required for raf binding and regulates MEK function. *Mol. Cell. Biol.* **15**, 5214-5225.

Coles, L. C. and Shaw, P. E. (2002). PAK1 primes MEK1 for phosphorylation by Raf-1 kinase during cross-cascade activation of the ERK pathway. *Oncogene* **21**, 2236-2244.

Crews, C. M., Alessandrini, A. and Erikson, R. L. (1992). The primary structure of MEK, a protein kinase that phosphorylates the ERK gene product. *Science* **258**, 478-480.

Cross, J. C. (2005). How to make a placenta: mechanisms of trophoblast cell differentiation in mice: a review. *Placenta* **26 Suppl. A**, S3-S9.

Cross, J. C., Nakano, H., Natale, D. R., Simmons, D. G. and Watson, E. D. (2006). Branching morphogenesis during development of placental villi. *Differentiation* **74**, 393-401.

Dang, A., Frost, J. A. and Cobb, M. H. (1998). The MEK1 proline-rich insert is required for efficient activation of the mitogen-activated protein kinases ERK1 and ERK2 in mammalian cells. *J. Biol. Chem.* **273**, 19909-19913.

Eblen, S. T., Slack, J. K., Weber, M. J. and Catling, A. D. (2002). Rac-PAK signaling stimulates extracellular signal-regulated kinase (ERK) activation by regulating formation of MEK1-ERK complexes. *Mol. Cell. Biol.* **22**, 6023-6033.

Eblen, S. T., Slack-Davis, J. K., Tarcsafalvi, A., Parsons, J. T., Weber, M. J. and Catling, A. D. (2004). Mitogen-activated protein kinase feedback phosphorylation regulates MEK1 complex formation and activation during cellular adhesion. *Mol. Cell. Biol.* **24**, 2308-2317.

Fischer, A. M., Katayama, C. D., Pages, G., Pouyssegur, J. and Hedrick, S. M. (2005). The role of erk1 and erk2 in multiple stages of T cell development. *Immunity* **23**, 431-443.

Foulds, C. E., Nelson, M. L., Blaszczak, A. G. and Graves, B. J. (2004). Ras/mitogen-activated protein kinase signaling activates Ets-1 and Ets-2 by CBP/p300 recruitment. *Mol. Cell. Biol.* **24**, 10954-10964.

Frost, J. A., Steen, H., Shapiro, P., Lewis, T., Ahn, N., Shaw, P. E. and Cobb, M. H. (1997). Cross-cascade activation of ERKs and ternary complex factors by Rho family proteins. *EMBO J.* **16**, 6426-6438.

Giroux, S. and Charron, J. (1998). Defective development of the embryonic liver in N-*myc*-deficient mice. *Dev. Biol.* **195**, 16-28.

Giroux, S., Tremblay, M., Bernard, D., Cardin-Girard, J. F., Aubry, S., Larouche, L., Rousseau, S., Huot, J., Landry, J., Jeannotte, L. et al. (1999). Embryonic death of Mek1-deficient mice reveals a role for this kinase in angiogenesis in the labyrinthine region of the placenta. *Curr. Biol.* **9**, 369-372.

Gopalbhai, K., Jansen, G., Beauregard, G., Whiteway, M., Dumas, F., Wu, C. and Meloche, S. (2003). Negative regulation of MAPKK by phosphorylation of a conserved serine residue equivalent to Ser212 of MEK1. *J. Biol. Chem.* **278**, 8118-8125.

Hayashi, S., Lewis, P., Pevny, L. and McMahon, A. P. (2002). Efficient gene modulation in mouse epiblast using a Sox2Cre transgenic mouse strain. *Gene Expr. Patterns* **2**, 93-97.

Hayashi, S., Tenzen, T. and McMahon, A. P. (2003). Maternal inheritance of Cre activity in a Sox2Cre deleter strain. *Genesis* **37**, 51-53.

Hayashi, Y., Koike, M., Matsutani, M. and Hoshino, T. (1988). Effects of fixation time and enzymatic digestion on immunohistochemical demonstration of bromodeoxyuridine in formalin-fixed, paraffin-embedded tissue. *J. Histochem. Cytochem.* **36**, 511-514.

Hsu, J. C. and Perrimon, N. (1994). A temperature-sensitive MEK mutation demonstrates the conservation of the signaling pathways activated by receptor tyrosine kinases. *Genes. Dev.* **8**, 2176-2187.

Jelinek, T., Catling, A. D., Reuter, C. W., Moodie, S. A., Wolfman, A. and Weber, M. J. (1994). RAS and RAF-1 form a signalling complex with MEK-1 but not MEK-2. *Mol. Cell. Biol.* **14**, 8212-8218.
Johnson, G. L. and Vaillancourt, R. R. (1994). Sequential protein kinase reactions controlling cell growth and differentiation. *Curr. Opin. Cell Biol.* **6**, 230-238.
Kornfeld, K., Guan, K. L. and Horvitz, H. R. (1995). The Caenorhabditis elegans gene mek-2 is required for vulval induction and encodes a protein similar to the protein kinase MEK. *Genes Dev.* **9**, 756-768.
Lendrum, A. C., Fraser, D. S., Slidders, W. and Henderson, R. (1962). Studies on the character and staining of fibrin. *J. Clin. Pathol.* **15**, 401-413.
Littell, R. C., Henry, P. R. and Ammerman, C. B. (1998). Statistical analysis of repeated measures data using SAS procedures. *J. Anim. Sci.* **76**, 1216-1231.
Nantel, A., Mohammad-Ali, K., Sherk, J., Posner, B. I. and Thomas, D. Y. (1998). Interaction of the Grb10 adapter protein with the Raf1 and MEK1 kinases. *J. Biol. Chem.* **273**, 10475-10484.
Pagon, Z., Volker, J., Cooper, G. M. and Hansen, U. (2003). Mammalian transcription factor LSF is a target of ERK signaling. *J. Cell Biochem.* **89**, 733-746.
Papin, C., Denouel, A., Calothy, G. and Eychene, A. (1996). Identification of signalling proteins interacting with B-Raf in the yeast two-hybrid system. *Oncogene.* **12**, 2213-2221.
Parekh, V., McEwen, A., Barbour, V., Takahashi, Y., Rehg, J. E., Jane, S. M. and Cunningham, J. M. (2004). Defective extraembryonic angiogenesis in mice lacking LBP-1a, a member of the grainyhead family of transcription factors. *Mol. Cell. Biol.* **24**, 7113-7129.
Park, E. R., Eblen, S. T. and Catling, A. D. (2007). MEK1 activation by PAK: a novel mechanism. *Cell. Signal.* **19**, 1488-1496.
Qian, X., Esteban, L., Vass, W. C., Upadhyaya, C., Papageorge, A. G., Yienger, K., Ward, J. M., Lowy, D. R. and Santos, E. (2000). The Sos1 and Sos2 Ras-specific exchange factors: differences in placental expression and signaling properties. *EMBO J.* **19**, 642-654.
Rubinfeld, H. and Seger, R. (2005). The ERK cascade: a prototype of MAPK signaling. *Mol. Biotechnol.* **31**, 151-174.
Russell, M., Lange-Carter, C. A. and Johnson, G. L. (1995). Regulation of recombinant MEK1 and MEK2b expressed in Escherichia coli. *Biochemistry* **34**, 6611-6615.
Sato, F., Yasumoto, K., Kimura, K., Numayama-Tsuruta, K. and Sogawa, K. (2005). Heterodimerization with LBP-1b is necessary for nuclear localization of LBP-1a and LBP-1c. *Genes Cells* **10**, 861-870.
Schaeffer, H. J., Catling, A. D., Eblen, S. T., Collier, L. S., Krauss, A. and Weber, M. J. (1998). MP1: A MEK binding partner that enhances enzymatic activation of the MAP kinase cascade. *Science* **281**, 1668-1671.
Schmitz, T., Souil, E., Herve, R., Nicco, C., Batteux, F., Germain, G., Cabrol, D., Evain-Brion, D., Leroy, M. J. and Mehats, C. (2007). PDE4 inhibition prevents preterm delivery induced by an intrauterine inflammation. *J. Immunol.* **178**, 1115-1121.
Schreiber, J., Riethmacher-Sonnenberg, E., Riethmacher, D., Tuerk, E. E., Enderich, J., Bosl, M. R. and Wegner, M. (2000). Placental failure in mice lacking the mammalian homolog of glial cells missing, GCMa. *Mol. Cell. Biol.* **20**, 2466-2474.
Seger, R. and Krebs, E. G. (1995). The MAPK signaling cascade. *FASEB. J.* **9**, 726-735.
Setalo, G., Jr, Singh, M., Guan, X. and Toran-Allerand, C. D. (2002). Estradiol-induced phosphorylation of ERK1/2 in explants of the mouse cerebral cortex: the roles of heat shock protein 90 (Hsp90) and MEK2. *J. Neurobiol.* **50**, 1-12.
Seufferlein, T., Withers, D. J. and Rozengurt, E. (1996). Reduced requirement of mitogen-activated protein kinase (MAPK) activity for entry into the S phase of the cell cycle in Swiss 3T3 fibroblasts stimulated by bombesin and insulin. *J. Biol. Chem.* **271**, 21471-21477.
Sharma, P., Veeranna Sharma, M., Amin, N. D., Sihag, R. K., Grant, P., Ahn, N., Kulkarni, A. B. and Pant, H. C. (2002). Phosphorylation of MEK1 by cdk5/p35 down-regulates the mitogen-activated protein kinase pathway. *J. Biol. Chem.* **277**, 528-534.
Simmons, D. G., Natale, D. R., Begay, V., Hughes, M., Leutz, A. and Cross, J. C. (2008). Early patterning of the chorion leads to the trilaminar trophoblast cell structure in the placental labyrinth. *Development* **135**, 2083-2091.
Skarpen, E., Flinder, L. I., Rosseland, C. M., Orstavik, S., Wierod, L., Oksvold, M. P., Skalhegg, B. S. and Huitfeldt, H. S. (2007). MEK1 and MEK2 regulate distinct functions by sorting ERK2 to different intracellular compartments. *FASEB J.* **2**, 466-476.
Soriano, P. (1999). Generalized lacZ expression with the ROSA26 Cre reporter strain. *Nat. Genet.* **21**, 70-71.
Stecca, B., Nait-Oumesmar, B., Kelley, K. A., Voss, A. K., Thomas, T. and Lazzarini, R. A. (2002). Gcm1 expression defines three stages of chorio-allantoic interaction during placental development. *Mech. Dev.* **115**, 27-34.
Umbhauer, M., Marshall, C. J., Mason, C. S., Old, R. W. and Smith, J. C. (1995). Mesoderm induction in Xenopus caused by activation of MAP kinase. *Nature* **376**, 58-62.
Ussar, S. and Voss, T. (2004). MEK1 and MEK2, different regulators of the G1/S transition. *J. Biol. Chem.* **279**, 43861-43869.
Volker, J. L., Rameh, L. E., Zhu, Q., DeCaprio, J. and Hansen, U. (1997). Mitogenic stimulation of resting T cells causes rapid phosphorylation of the transcription factor LSF and increased DNA-binding activity. *Genes Dev.* **11**, 1435-1446.
Winston, B. W., Remigio, L. K. and Riches, D. W. (1995). Preferential involvement of MEK1 in the tumor necrosis factor-alpha-induced activation of p42mapk/erk2 in mouse macrophages. *J. Biol. Chem.* **270**, 27391-27394.
Wu, X., Noh, S. J., Zhou, G., Dixon, J. E. and Guan, K. L. (1996). Selective activation of MEK1 but not MEK2 by A-Raf from epidermal growth factor-stimulated Hela cells. *J. Biol. Chem.* **271**, 3265-3271.
Wu, Y., Han, M. and Guan, K. L. (1995). MEK-2, a Caenorhabditis elegans MAP kinase kinase, functions in Ras-mediated vulval induction and other developmental events. *Genes Dev.* **9**, 742-755.
Xu, S., Khoo, S., Dang, A., Witt, S., Do, V., Zhen, E., Schaefer, E. M. and Cobb, M. H. (1997). Differential regulation of mitogen-activated protein/ERK kinase (MEK)1 and MEK2 and activation by a Ras-independent mechanism. *Mol. Endocrinol.* **11**, 1618-1625.
Zheng, C. F. and Guan, K. L. (1993). Properties of MEKs, the kinases that phosphorylate and activate the extracellular signal-regulated kinases. *J. Biol. Chem.* **268**, 23933-23939.